Prediction of Boundary Layer Transition at High Freestream Turbulence Conditions, Using a Physical Model

R. Tagavi-Zenouz[1], M. Salari[2]
Mech. Eng. Dep't., Iran Univ. of Science and Tech.

ABSTRACT
A physical model, based on modeling of the near wall velocity fluctuations, is used for prediction of transition in an attached boundary layer. The near wall velocity fluctuations are assumed to develop into turbulent spots when their amplitudes, exceed a threshold value. In this work, the relevant physical correlations are developed and incorporated in a conventional boundary layer computer code for prediction of transitional flows. Test cases include transitional flat plate boundary layer flows under zero and non-zero pressure gradients with various freestream turbulence intensities. The results show close agreements with available experimental data.

Key Words: Boundary Layer Transition, Laminar Flow Fluctuations, Transition Modeling, Physical Model.

پیش‌بینی گذار در لایه مرزی جریان‌های با شدت توربولانسی زیاد جریان آزاد به کمک یک مدل فیزیکی

رضا تقوی زنوز و محمود سالاری
دانشکده مهندسی مکانیک، دانشگاه علم وصنعت ایران

چکیده
در مقاله حاضر از یک مدل فیزیکی، که اساس آن بر مدلسازی نوسانات سرعت نزدیک دیواره جریان های لایه مرزی استوار است، برای پیش بینی فرایند گذار، درجریان های با لایه مرزی چسبیده به سطح استفاده شده است. این مدل فرض می کند تولید و رشد نقطه های توربولانسی در ناحیه لایه ای جریان زمانی آغاز می شود که دامنه نوسانات سرعت نزدیک دیواره از مقدار معینی بیشتر شود. در این تحقیق، روابط فیزیکی حاکم بر رفتار پارامترهای ناحیه گذار بسط داده شده و بر مبنای آن یک نرم افزار رایانه ای لایه مرزی تهیه شده است. به کمک این نرم افزار، رفتار تعدادی از جریان های در حال گذار مطالعه شده است. جریان های مطالعه شده در این مقاله شامل جریان های لایه مرزی در حال گذار تحت شرایط گرادیان فشار صفر و غیر صفر می باشد که در آنها شدت توربولانس جریان آزاد دارای مقادیر متفاوت و بالایی است. نتایج حاصل تطبیق مناسبی را با داده های تجربی نشان می دهد.

واژه های کلیدی : لایه مرزی در حال گذار، نوسانات ناحیه لایه ای، مدلسازی فرایند گذار

1 - Assistant Prof.: Taghavi@iust.ac.ir

2 - PhD Student (Corresponding Author): m_salari@iust.ac.ir

Nomenclature

a, b, c	Empirical Constants in Equation (1)
f	Frequency Fluctuation
u	Local Time Mean Velocity
U	Freestream Time Mean Velocity
$\overline{u'_f}$	Local R.M.S. Velocity in a Particular Frequency Band
$\overline{U'_f}$	Freestream R.M.S. Velocity in a Particular Frequency Band
u'_m	Local Fluctuating Velocity Minima
L	Near Wall Integral Length Scale
L	Freestream Integral Length Scale
δ^*	Displacement Thickness
δ	Boundary Layer Thickness
θ	Momentum Thickness
λ	Pohlhausen Parameter
x	Streamwise Distance from Leading Edge
Re_L	Reynolds Number Based on Freestream Integral Length Scale
H	Shape Factor
Tu	Freestram Turbulence Level
C_f	Skin Friction Coefficient

1. Introduction

Boundary layer transition is significant to many flow fields that include both laminar and turbulent regions. Accurate prediction of transition onset is fundamental to the modeling of these flows. Distributions of pressure, wall shear stress and heat transfer rate over solid walls are strongly dependent on location of commencement of transition. In addition, length of transitional zone and flow properties within this region, are also of great importance, which need to be studied carefully. Of the examples in which the transitional flows have dominant effects can be referred to all external surfaces of flying objects, like wings and bodies, and also compressor and turbine blades in turbomachines.

There are different transition mechanisms, which are basically dependent on external flow turbulence intensity level, streamwise pressure gradient, solid wall geometry and surface roughness [1]. Mayle[2] has identified two distinct transition mechanisms for attached boundary layers. In one mechanism, transition occurs at freestream turbulence levels of less than about 1%, which is due to amplification of Tollmien-Schlichting (T-S) waves. This type of transition is so-called "natural transition". In this case, if amplitudes of the T-S waves are large enough, each cycle of the wave results in generation of a single turbulent spot. Based on this assumption, Walker and Gostelow[3] determined initially a minimum possible length for transitional region. Then, its actual total length was approximated, by multiplying this minimum length by an empirical factor, which is greater than unity. This was performed due to the fact that not all cycles of the T-S waves would have sufficient amplitude to initiate a turbulent spot.

For the second transition mechanism, which occurs at higher freestream turbulence levels, there is little evidence of the T-S waves. The linear growth of T-S waves is bypassed and transition takes place through a mechanism called "bypass transition". This type of transition is a complex phenomenon, which depends mainly on the turbulence intensity and the status of the boundary layer such as pressure gradient, separation and so on [2, 4].

It is clear that, a complete spectrum of frequencies can be detected within boundary layers subjected to higher free stream turbulence intensities, and a single T-S frequency is not observed. Similar to the Walker's[3] transition model for low freestream turbulence intensities, Johnson[5] proposed an extended model for prediction of transition in high freestream turbulence intensity levels. It is assumed in this model that every minimum of sufficient amplitude of turbulence level would initiate a turbulent spot.

The objective of the current work is to develop and evaluate the physical model of Johnson [5], for prediction of some transitional boundary layer flows. In this research, the relevant correlations are developed and incorporated into a boundary layer computerized code for studying the transition phenomenon in the attached flows. The numerical results are compared with available experimental data. The results show the model is more effective for high levels of turbulence intensities, i.e., the bypass transition.

2. Concepts

Mayle [2] showed that the freestream turbulence level and pressure gradient have the most dominant influences on the location of commencement of transition and its length. The concepts of the transition model that are introduced in the current study are based on the physical effects of freestream turbulence on the boundary layer transition.

DNS calculations of Voke [6] show that a turbulent spot is initiated in a laminar boundary layer when a local instantaneous flow separation occurs on the solid wall. It can be shown, from the DNS results that a local separation of the flow takes place when the local instantaneous velocity in the near wall region drops below 50% of the local time mean velocity. Mayle and Schulz [4] demonstrated that the near wall velocity fluctuations depend primarily on the freestream local turbulence and pressure gradient. They suggested that a more plausible mechanism than convection or diffusion for production of the near wall velocity perturbations is the unsteady pressure field, which is generated by the freestream turbulence.

Based on the above observations, Johnson and Ercan [7] proposed that the turbulence spot formation rate can be predicted if statistical information on the number and depth of the minima (i.e., every minimum of sufficient amplitudes of the Walker's model) within the near wall velocity signal could be derived. Therefore, they studied experimentally the response of laminar boundary layers to different freestream turbulences. The measurements of turbulence intensity amplification (i.e., the ratio between near wall and freestream turbulence levels for a particular frequency) through a typical laminar boundary layer for six frequency bands are plotted in Fig.1 where, U_{y0} and δ are velocity gradient in wall and boundary layer thickness, respectively. It can be detected from Fig.1 that the boundary layer has a selectivity manner to certain freestream eddy scales, so the low-frequency disturbances (i.e. larger freestream turbulent wavelengths) are more amplified by the mean shear in the boundary layer. It also indicates that these low frequencies become dominant in the velocity signal close to the wall. The other noticeable feature is that the spectra are invariant for y/δ values up to approximately 0.3, so this region will be referred to as the "near-wall region" in the context. The experimental results of the near wall gain are shown for a number of different zero pressure gradient boundary layers in Figure **2**. For dimensionless frequencies greater than 0.1 the results are very similar, but for low frequencies the ratio increases with decreasing the skin friction coefficient, C_f.

3. Formulation of Transition Model

Experimental results of the near wall amplification ratio, G, shown already in

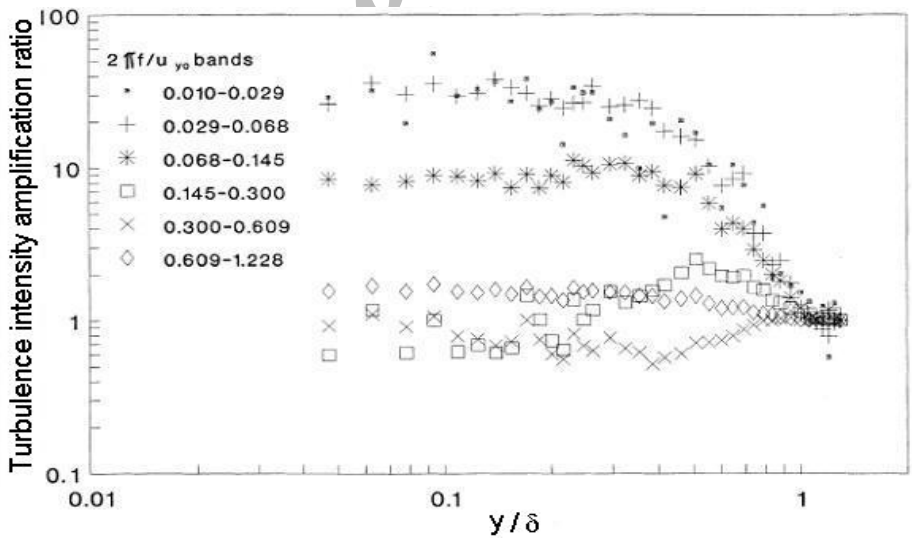

Figure 1. Amplification of six frequency bands through a laminar boundary layer [7].

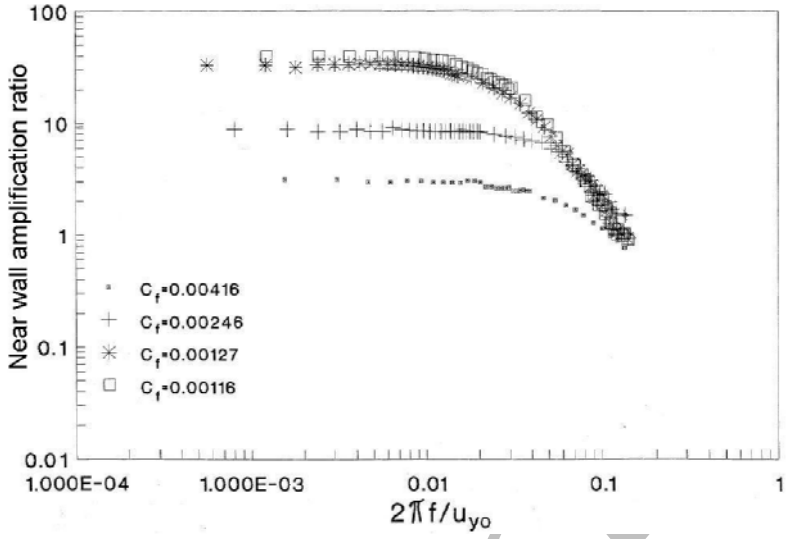

Figure 2. Near wall amplification as a function of frequency [7].

Figure **2** can be reasonably represented by the following relation:

$$G = \left(\overline{u'_f}/\overline{U'_f}\right)\Big/(u/U) = \frac{a}{C_f^c + \left(2\pi.b.f/u_{y0}\right)^2} \quad . \qquad (1)$$

Equation (1) is derived based on application of well-known least square curve fitting technique using available experimental data, already presented in Fig. 2. The constants appeared in Eq. (1) are obtained as follows:

$$a = 1.595\times10^{-4}, b = 0.015, c = 1.827.$$

The curves obtained through Equation (1) are superimposed in Figure **2** and all are shown again in Figure **3**. Assuming the freestream turbulence fluctuations are isotropic, Power spectral density, E, can be represented, Hinze [8], by the following equation:

$$E = \frac{4\overline{U'}^2 L}{U\left(1+(2\pi fL/U)^2\right)}, \qquad (2)$$

where, L is the free stream integral length scale.
The near wall spectral density, e, is then given by:

$$e = \left(\frac{\overline{u'_f}}{\overline{U'_f}}\right)^2 E = G^2\left(\frac{\overline{U'}}{U}\right)^2\left(\frac{u}{U}\right)^2 \frac{4UL}{\left(1+(2\pi fL/U)^2\right)} \quad . \qquad (3)$$

Hence, the near wall local turbulence level, $Tu_{NW,}$ can be represented by:

$$Tu_{NW}^2 = \int_0^\infty \frac{edf}{u^2}, = \frac{4a^2.Tu^2}{C_f^{2c}}\int_0^\infty \frac{dF}{\left(1+(BF)^2\right)^2(1+F^2)}, \qquad (4)$$

where,

$$F = \frac{2\pi fL}{u}, B = \frac{2.b}{\mathrm{Re}_L.C_f^{\left(1+c/2\right)}}.$$

The ratio of near wall to freestream turbulence levels can be shown by:

$$\left(\frac{Tu_{NW}}{Tu}\right) = \frac{a}{C_f^c}(B+1)\left(\frac{B}{2}+1\right)^{1/2} \quad . \qquad (5)$$

It can be shown that if B is small, less than approximately 0.1, the above ratio will be independent of the freestream length scale, L, and Equation (5) can be simplified as Equation (6).

$$\left(\frac{Tu_{NW}}{Tu}\right) = \frac{a}{C_f^c} \qquad (6)$$

The above simplification can be performed for high free stream turbulence levels where both the length scale, L, and C_f are comparatively large and consequently B is small. Fig**. 4** confirms the above conclusion, as the high free stream turbulence intensity results fall close to a single line represented by Equation (6).

3.1. Near Wall Velocity Signal

The near wall integral length scale, l, is evaluated from its definition through the following equation:

$$\int_0^{U/l} edf = 0.5\int_0^{\infty} edf \,. \qquad (7)$$

Substituting for, e, from Equation (3) and integrating, one obtains:

$$\frac{2}{\pi}\frac{2}{B^2-1}(0.25\sin 2\phi + 0.5\phi) + \frac{2}{\pi(B^2-1)^2} \times (\arctan(L/l) - B\phi) = \frac{B+2}{4(B+1)^2} \qquad (8)$$

where,

$$\phi = \arctan(BL/l)\,.$$

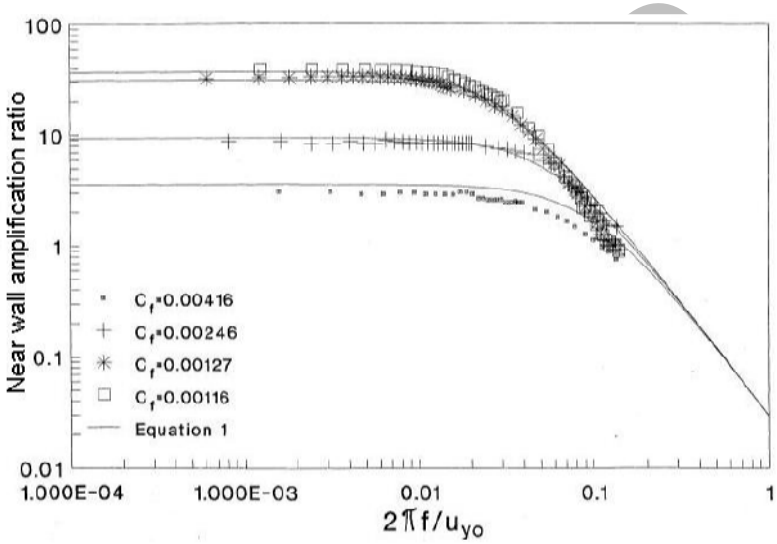

Figure 3. Curve fitting of the experimental results of the near wall amplification

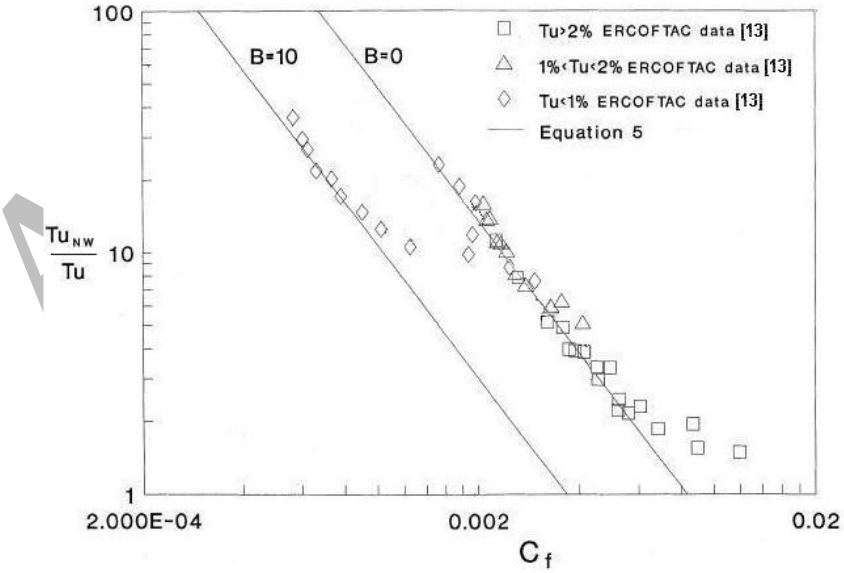

Figure 4. Ratio of near wall to freestream turbulence levels for favorable, zero and adverse pressure gradient laminar boundary layers.

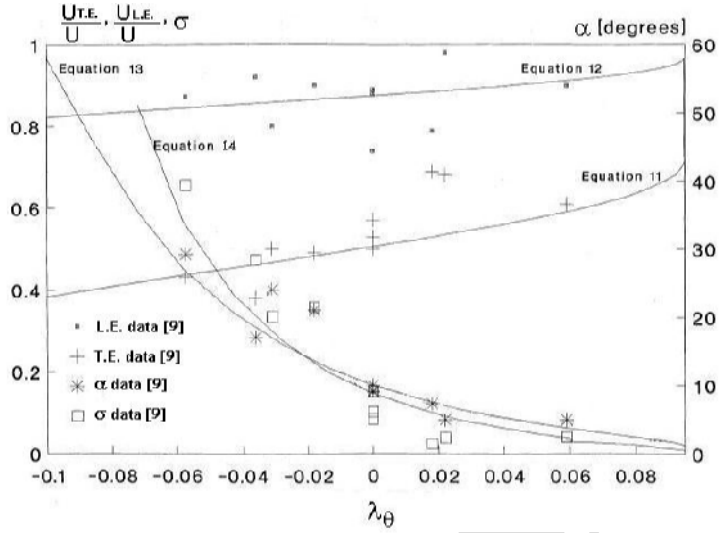

Figure 5. Comparison of the relations of spot trailing and leading edge velocities, spreading half angle and propagation parameter with experimental data.

The above equation can be solved numerically to obtain *l*/L for any value of B. The near wall velocity signal can be synthesized from the power spectral density, *e*, for a range of B values. Johnson et al. [7] analyzed the near wall velocity signals to obtain statistical information for the minima (i.e., every minimum of sufficient amplitude of turbulence level that initiate a turbulent spot). They obtained the following correlation for the number of minima per local wavelength, z, as a function of the length scale ratio (*l*/L):

$$z = 3.2 - 2.5\exp(-0.043 l / L) \quad . \qquad (9)$$

They also showed that the instantaneous velocities have a normal distribution about the mean value and the minima have a distribution as: $\left(\frac{u'_m}{\overline{u'}}\right)\exp\left(-0.5\left(\frac{u'_m}{\overline{u'}}\right)^2\right)$. If Voke's [6] criterion is now adopted, i.e., any minima where $u'_m/u < 0.5$ will lead to the generation of a turbulent spot, it follows that the proportion of minima, P, which will generate spots is given by:

$$P = \frac{1}{4}\sqrt{\frac{1}{2\pi}}\int_{\infty}^{u/2\overline{u'}}\left(\frac{u}{\overline{u'}}\right)^2 \exp\left(-\frac{1}{8}\left(\frac{u}{\overline{u'}}\right)^2\right) d\left(\frac{u}{\overline{u'}}\right) \quad .$$

Assuming the freestream turbulence is convected at the freestream velocity U, then the spot generation rate per unit time per unit area of the surface would be specified as $PU(z/l)^3$ [7].

3.2. Turbulent Spot Development

If the laminar boundary layer is assumed to have a Pohlhausen velocity profile as:

$$\frac{u}{U} = 2\left(\frac{y}{\delta}\right) - 2\left(\frac{y}{\delta}\right)^3 + \left(\frac{y}{\delta}\right)^4 + \frac{\lambda}{6}\left(\frac{y}{\delta}\right)\left(1 - \frac{y}{\delta}\right)^3 ,$$

the trailing and leading edge velocities (U_{TE}, U_{LE}) of a turbulent spot can be represented, in comparison with experimental data of Gostelw's [9], by the velocities existing at y/δ= 0.27 and 0.57, respectively. Therefore:

$$\frac{U_{TE}}{U} = 0.506 + 0.0175\lambda \quad , \qquad (11)$$

$$\frac{U_{LE}}{U} = 0.875 + 0.00755\lambda \quad , \qquad (12)$$

where $\lambda = \lambda_\theta\left(\theta/\delta\right)^2$ is the Pohlhausen parameter. The spreading half angle, α, of the turbulent spot can also be represented by:

$$\alpha = Tan^{-1}\left(\frac{0.242\left(U_{LE} - U_{TE}\right)}{U_{TE}\left(1 - \lambda/12\right)^2}\right) \quad . \qquad (13)$$

The propagation parameter σ can then be evaluated as the following relation:

$$\sigma = \left(\frac{U}{U_{TE}} - \frac{U}{U_{LE}} \right) Tan(\alpha) . \qquad (14)$$

As shown in Figure **5**, the comparisons of parameters introduced by the above equations with the experimental results of Gostelow et al [9] show good agreements.

3.3. Intermittency

The intermittency at a point is defined as the proportion of time, which the flow is turbulent at that point within a specified period. For a two dimensional boundary layer however it is also equal to the proportion of a spanwise line, which passes through the same point, and is occupied by turbulent flow at a particular instant. Consider such a spanwise line is traveling downstream at the local spot trailing edge velocity U_{TE}. Figure **6** shows that any spots initiated in the shaded x-t window will cross the span-wise line as it travels downstream through the distance Δx. It therefore follows that the spot generation rate per unit span can be represented by [7]:

$$\frac{dN}{dt} = (1-\gamma)\left(\frac{U_{LE} - U_{TE}}{U_{LE}} \right) \int_0^x PU \left(\frac{z}{l} \right)^3 dx - \frac{2U_{TE} N^2 Tan(\alpha)}{1-\gamma} . \qquad (15)$$

The first term in this equation represents the rate at which spots generated upstream arrive at laminar regions on the line. The second term represents the rate at which spots already on the line merge. The increase in intermittency is due to lateral spreading of spots on the line. Thus, substituting Equation (13) for α and the following relations:

$$\frac{d\gamma}{dt} = 2N.U_{TE} Tan(\alpha) , \qquad (16)$$

$$\frac{dx}{dt} = U_{TE} ,$$

for the spanwise line, results in:

$$\frac{dN}{dx} = \frac{(1-\gamma)\sigma}{U.Tan(\alpha)} \int_0^x P.U \left(\frac{z}{l} \right)^3 dx - \frac{2N^2 Tan(\alpha)}{(1-\gamma)}, \qquad (17)$$

and

$$\frac{d\gamma}{dx} = 2N.Tan(\alpha) . \qquad (18)$$

It should be noted, the Equation (17) and (18) are consistent with the frequently adopted Narasimha [10] intermittency model.

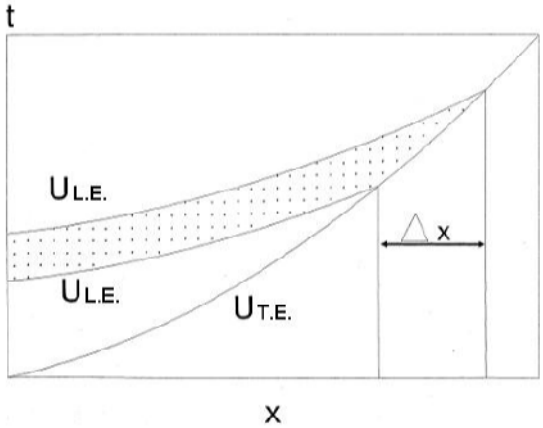

Figure 6. Spot generation window for spanwise line traveling downstream at U_{TE} [7].

4. Boundary Layer Integral Technique

In the current work, the relevant physical correlations are incorporated in a conventional boundary layer code and used for prediction of some transitional flows.

The development of the boundary layer is computed through numerical integration of the boundary layer momentum equation in the streamwise direction, introduced as Equation (19).

$$\frac{d\theta}{dx} = \frac{C_f}{2} - \left(\frac{2\theta + \delta^*}{U} \right) \frac{dU}{dx} \qquad (19)$$

The laminar and turbulent portions of the boundary layer are integrated separately and the integral parameters are evaluated as intermittency weighted averages of the laminar and turbulent values, so

$$C_f = (1-\gamma) C_{fl} + \gamma C_{ft} ,$$

$$\mathrm{Re}_{\delta^*} = (1-\gamma)\,\mathrm{Re}_{\delta^* l} + \gamma\,\mathrm{Re}_{\delta^* t} , \qquad (20)$$

$$\mathrm{Re}_{\theta} = (1-\gamma)\,\mathrm{Re}_{\theta l} + \gamma\,\mathrm{Re}_{\theta t} .$$

The intermittency γ is obtained by numerical integration of Equation (17) and (18). The laminar boundary layer is assumed to have a Pohlhausen profile, as:

$$\frac{u}{U} = 2\frac{y}{\delta} - 2\left(\frac{y}{\delta} \right)^3 + \left(\frac{y}{\delta} \right)^4 + \frac{\lambda}{6}\left[\left(\frac{y}{\delta} \right) - 3\left(\frac{y}{\delta} \right)^2 + 3\left(\frac{y}{\delta} \right)^3 - \left(\frac{y}{\delta} \right)^4 \right] . \qquad (21)$$

Thus,

$$\frac{\theta}{\delta} = \frac{37}{315} - \frac{\lambda}{945} - \frac{\lambda^2}{9072}, \quad (22)$$

and

$$\frac{\delta^*}{\delta} = \frac{3}{10} - \frac{\lambda}{120}. \quad (23)$$

If the laminar boundary layer separates, the Pohlhausen parameter, λ, is kept constant as 0.12 downstream of the separation point. There is a similar technique adopted successfully by Solomon [11] for separated laminar flow. When a laminar portion of the boundary layer becomes turbulent, then it follows from the conservation of momentum that:

$$\theta_l = \theta_t \quad . \quad (24)$$

The turbulent boundary layer integral parameters C_f, Re_θ, and H were evaluated using the Ludwieg and Tillman [12], as:

$$C_f = 0.246.(10)^{-0.678H}\ \mathrm{Re}_\theta^{-0.268} \quad , \quad (25)$$

and Goksel [14], as:

$$\ln\left(\frac{H}{H-1}\right) = 0.1016 \ln \mathrm{Re}_\theta + 0.4822 \, . \quad (26)$$

5. Results and Discussion

Test cases selected for the current study are those performed experimentally by Savill [13], which are conducted by ERCOFTAC institute. These tests are focused on two- dimensional transitional boundary layers developing on a flat plate. The first three cases (T3A-, T3A and T3B) were set for nominally zero pressure gradients and three freestream turbulence levels of 1%, 3% and 6%, respectively. The remaining five test cases were set for a specified pressure distribution along a flat plate, typical of a loaded gas turbine blade. In the first case of this set of experiments (T3C1), the freestream turbulence level was 5%. For T3C2 to T3C5, where the turbulence level was 2.5%, the tunnel velocity was progressively reduced such that the transition location moved along the plate from the favorable pressure gradient region into the adverse pressure gradient region. Initial values of velocity, U_0, freestream turbulence level, FST, and turbulent integral length scale for these experimental cases are given in table 1.

The model used in the present study requires also the knowledge of both the freestream turbulence level and its integral length scale.

5.1 Zero Pressure Gradient Cases

The model predictions and measured values of skin friction coefficient, Cf, and shape factor, H, of T3A- test case are shown in Figures **7** and **8**, respectively.

Table 1. Initial flow parameters at the leading edge of ERCOFTAC [13] test cases.

Test Case	U0 (m/s)	FST (%)	Turbulent integral length scale	Pressure gradient
T3A-	19.8	0.9	2.0 mm	Zero
T3A	5.4	3.0	9.0 mm	Zero
T3B	9.4	6.0	12.5 mm	Zero
T3C1	5.9	6.6	6.5 mm	Non-zero
T3C2	5.0	3.0	6.5 mm	Non-zero
T3C3	3.7	3.0	6.5 mm	Non-zero
T3C4	1.2	3.0	6.5 mm	Non-zero
T3C5	8.4	3.0	6.5 mm	Non-zero

It can be seen that the onset of transition is predicted numerically to start at Re_x = 800,000, whereas, it is observed experimentally to begin at Re_x =1,300,000. This discrepancy can be explained as follows. For this test case, the integral length scale at the beginning of transition is almost equal to the boundary layer thickness. Earlier in this paper was shown that the boundary layer is most receptive to larger freestream turbulent wavelengths. It therefore follows that, in this test case, transition results from the strong amplification of the longest wavelengths in the freestream, which here make up only a small proportion of the freestream turbulent energy. This can be demonstrated by decreasing the freestream integral length scale (by 40%) as shown in figure **7**. This decreases the proportion of long wavelengths in the freestream and, as shown in figure **7**, moves the position of transition commencement point downstream close to that detected experimentally. It should be noted that although this procedure improves the accuracy of the results, but it should be noted that a similar improvement could also be obtained by necessary changes to the empirical constants, which are already used for prediction of the transition receptivity to low frequencies.

The model predictions for skin friction coefficient and the shape factor for T3A test case are also compared with the experimental data in Figures **7** and **8**. It can be seen that the numerical predictions are fairly close to the measured values. However, the experiments show a decrease in H prior to start of transition, whereas, the predictions maintain the Blasius's H value of about 2.5. Similar reductions in H due to increase in freestream turbulence level have been observed by several researchers (e.g., Johnson [5], Gostelow et al. [15]), which are believed to be due to enhanced mixing within the laminar boundary layer. Commencement point of transition is predicted slightly earlier, but the transition length is very close to the measured value. The integral length scale of 9.0 mm is approximately twice the boundary layer thickness at the start point of transition. The boundary layer is therefore receptive to the majority of the freestream turbulent frequencies and so the transition location is fairly insensitive to the integral length scale.

The integral length scale of T3B test case is six times the boundary layer thickness at the beginning of transition. The transition location will therefore be unaffected by significant changes in the length scale. The computational results shown in figure **7** show that the location of the minimum C_f is predicted further down, but once again the transition length is well determined.

5.2 Non-zero pressure gradient cases

Fig. **9** shows the distribution of pressure coefficient along the flat plate for all ERCOFTAC [13] T3C test cases. For these casess, the pressure gradient is initially negative (favourable) and then positive (adverse) in a profile that was designed to roughly approximate the flow over a turbine blade. The mesh screen used in the T3B test case was also used in the T3C1 test case to induce a turbulence intensity level of approximately 5%. The current computational results and the experimental results of T3C1 case are presented in Fig. 10, which show reasonable agreement.

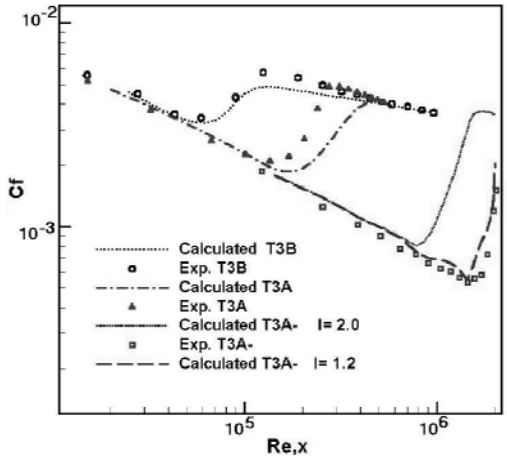

Figure 7. Experimental and numerical results of skin friction coefficients for the T3A-, T3A and T3B test cases under zero streamwise pressure gradient.

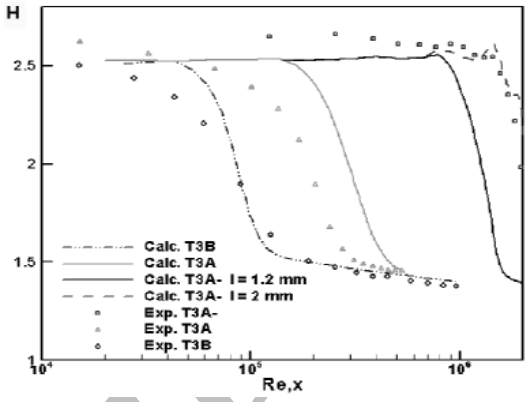

Figure 8. Experimental and numerical results of shape factor for the T3A-, T3A and T3B test cases under zero streamwise pressure gradient.

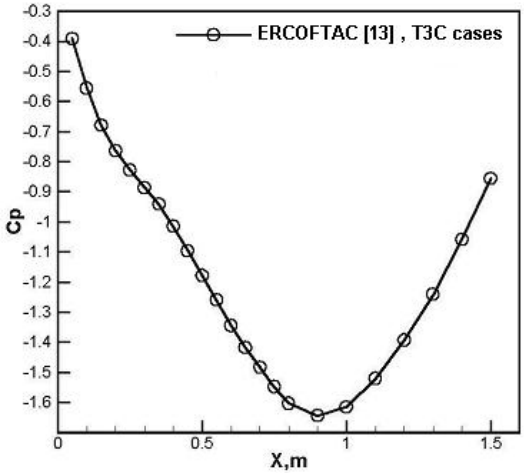

Figure 9. Distribution of pressure coefficient along the flat plate for all T3C test cases.

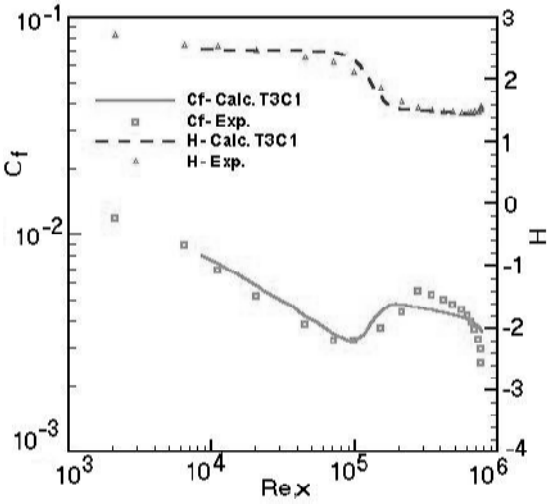

Figure 10. Numerical and experimental results of C_f and H for the T3C1 test case.

It can be detected through comparison of Figures **7** and **10** that the favorable pressure gradient has the effect of delaying the predicted minimum C_f location from Re_x = 62,000 for T3B test case to 100,000 in this case.

The remaining four test cases are for nominal freestream turbulence level of 2.5% induced by the T3A turbulence generator mesh screen. The pressure coefficient distribution is the same as for T3C1 test case, but the tunnel speed is progressively reduced through cases T3C5, T3C2, T3C3 and T3C4, which have the effect of shifting the transition further downstream. The relevant results are shown in figure **11**. For the T3C5 case, transition occurs within the favorable pressure gradient region and so the minimum C_f location is delayed up to Re_x=230,000 compared with Re_x=120,000 for the zero pressure gradient of T3A test case also figure **7**.

The tunnel wind velocity has been reduced in case T3C2 such that although transition inception occurs within the favorable pressure gradient region, but it is only completed once the pressure gradient has become adverse. Fig. **11** shows that the minimum C_f location is predicted at Re_x= 520,000, whereas the experimental
observations indicate that it occurs at about Re_x= 430,000. Shape factor results are shown in Fig. **12**. It can be detected from Figures **11** and **12** that when the laminar boundary layer is exposed to the adverse pressure gradient at Re_x= 470,000, the predicted value of C_f drops rapidly and H increases.

For T3C3 test case the commencement of transition is observed early in the adverse pressure gradient region and transition is still not completed up to the end of the plate. Fig. 11 shows that the boundary layer approaches laminar separation before the minimum C_f is achieved at Re_x=420,000, which is close to the experimental result. The predicted transition process proceeds more rapidly than that observed experimentally, however it ends prior to the tailing edge of the plate.

For T3C4 test case, the transitional boundary layer separates at Re_x=1.5 $\times 10^5$ before reattaching as a turbulent boundary layer at Re_x=1.8 $\times 10^5$ Figures **11** and **12**. The current integral method is incapable of correctly predicting the boundary layer development beyond laminar separation. However, the minimum C_f value and the subsequent rise through transition are predicted fairly well.

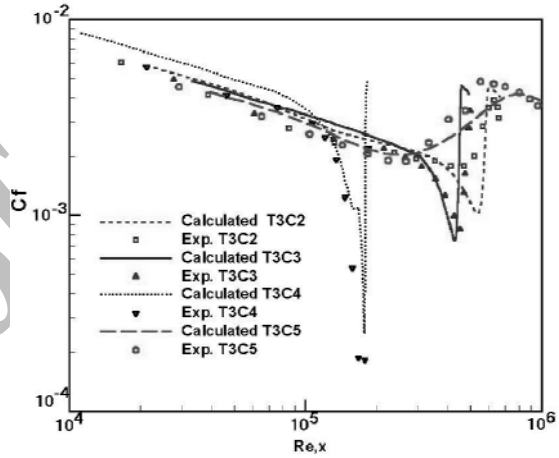

Figure 11. Numerical and experimental skin friction coefficient results for the T3C2, T3C3, T3C4 and T3C5 test cases

6. Conclusions

The current study shows that the proposed theoretical modeling of the near wall fluctuations is suitably capable of predicting the commencement of transition and its length. Our results are very close to those of available experimental ones, particularly at higher free stream turbulence levels, in which the bypass transition takes place. The over-prediction of transition length at Tu < 1.5% is most likely to be due to appearance of Tollmien- Schlichting waves, for in is not accounted within the current model. It can also be detected that at low turbulence levels, where the integral length scale is close to the magnitude of the boundary layer thickness, the transition length and its location are highly dependent on the integral length scale [16]. For the moderate turbulence levels, where the integral length scale is approximately twice the boundary layer thickness, the transition is only moderately sensitive to length scale. At higher

turbulence levels, the transition process is independent of the length scale, which is now many times larger than the boundary layer thickness.

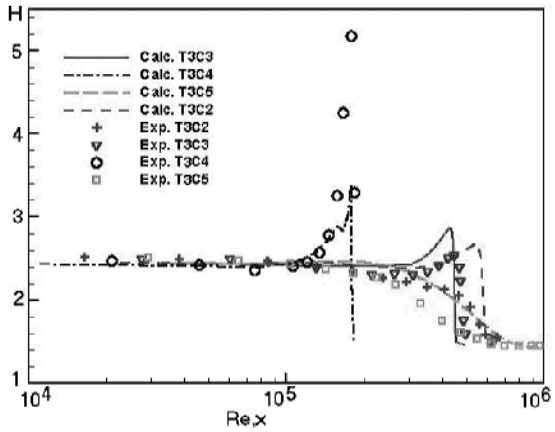

Figure 12. Numerical and experimental shape factor results for the T3C2, T3C3, T3C4 and T3C5 test cases.

7. References

1. Menter, F.R., Esch, T., and Kubacki, S., "Transition Modeling Based on Local Variables", The 5th Int. Symp. on Turbulence Modeling and Measurements, Mallorca, Spain, 2002.
2. Mayle, R.E., "The Role of Laminar-Turbulent Transition in Gas Turbine Engines", ASME J. Turbomach. Vol. 113, pp. 509-537, 1991.
3. Walker, G.J. and Gostelow, J.P., "Effects of Adverse Pressure Gradients on The Nature and Length of Boundary Layer Transition", ASME J. Turbomach. Vol. 112, 196-205, pp 1990.
4. Mayle, R.E., Schulz, A., "The Path to Predicting Bypass Transition", ASME Paper 96-GT-199, 1996.
5. Johnson, M.W., "A Bypass Transition Model for Boundary Layers", ASME J. Turbomach. Vol. 116, pp. 759-764, 1994.
6. Voke, P.R., "Laminar/Turbulent Transition of Boundary Layer Influenced by Freestream Disturbances", Euromech 330, Prague, 1995.
7. Johnson, M.W., and Ercan, A.H., "A Physical Model for Bypass Transition", Int. J. Heat Fluid Flow, Vol. 20, pp. 95–104, 1999.
8. Hinze, J.O., "Turbulence: Introduction to Its Mechanism and Theory", McGraw Hill, New York, 1959.
9. Gostelow, J.P., Melwani, N., Walker, G.J., "Effects of Streamwise Pressure Gradient on Turbulent Spot Development", ASME J. Turbomach. Vol. 118, pp. 737-743, 1995.
10. Narasimha, R., "The Laminar-Turbulent Transition Zone in The Boundary Layer", Prog. in Aerospace Science, Vol. 22, pp.29-80, 1985.
11. Solomon, W.J., Walker, G.J. and Gostelow, J.P., "Transition Length Prediction for Flows with Rapidly Changing Pressure Gradients", ASME J. Turbomach. Vol. 118, pp.185-209, 1995.
12. Ludwieg, H., Tillman, W., "Investigation of the Wall Shear Stress in Turbulent Boundary Layers", NACA T.N. 1284, 1950.
13. Savill, A.M., "A Synthesis of T3 Test Case Predictions", The 1st ERCOFTAC Workshop, Cambridge University Press, Cambridge, 1991.
14. Goksel, O.T., "Some Effects of Spherical Roughness Upon the Incompressible Flow of a Boundary Layer with Zero Pressure Gradient", Ph.D. Dissestation, Univ. of Liverpool, 1968.
15. Gostelow, J.P., Hong, G., Walker, G.J. and Dey, J., "Modeling of Boundary Layer Transition in Turbulent Flows by Linear Combination Integral Method", ASME Paper No. 94-GT-358, 1994.
16. Sohn, K.H., DeWitt, K.J., and Shyne, R.J., ''Experimental Investigation of Boundary Layer Behavior in a Simulated Low Pressure Turbine'', ASME J. Fluids Eng., Vol. 122, pp. 84–89, 2001.